EMERGENCE OF CIRCUMPOLAR VORTEX IN TWO DIMENSIONAL TURBULENCE ON A ROTATING SPHERE

Y.-Y. HAYASHI

Division of Earth and Planetary Sciences, Hokkaido University
Sapporo 060-0810, JAPAN

K. ISHIOKA AND M. YAMADA

Graduate School of Mathematical Sciences, University of Tokyo
Tokyo 153-8914, JAPAN

AND

S. YODEN

Department of Geophysics, Kyoto University
Kyoto, 606-8502, JAPAN

Abstract.

Characteristics of the decaying non-divergent two dimensional turbulence on a rotating sphere is considered. The spontaneous appearance of circumpolar easterly vortices reported in the previous study (Yoden and Yamada, 1993) is interpreted by the Rossby wave property from the framework of weak-nonlinear theory. The resolution of the numerical model utilized by Yoden and Yamada (1993) is T85 which is the resolution not enough to represent the upward energy cascade of two dimensional turbulence. The initial energy spectral peak adapted there is located almost in the range of wave regime especially when the rotation rate is large, which justifies the explanation of angular momentum redistribution by Rossby waves. A series of new experiments with the higher resolution T341 and new sets of initial energy spectral distributions are performed to confirm that the circumpolar vortices appear even after the full nonlinear upward cascade of turbulent energy and that the band structure of angular momentum emerges even when the rotation rate of the system is large.

1. Introduction

It has been recognized that a two dimensional turbulent flow on a rotating sphere tends to have a zonally band structure, i.e., bands of mean zonal flow with alternating flow direction. The pioneering work of this issue is Williams (1978), where a time evolution of a randomly forced two dimensional nondivergent fluid was numerically investigated to show that a zonally band structure emerges when the rotation rate and the radius of the sphere were adapted from those of Jupiter's. However, the computational domain utilized by Williams (1978) was only 1/16 of the entire sphere. The longitudinal periodicity and equatorial symmetry were assumed.

A full spherical computation of two dimensional turbulence on a sphere was rather recently carried out by Yoden and Yamada (1993, hereafter referred to as YY93). They investigated decaying, in stead of forced, two dimensional nondivergent turbulent flow on a rotating sphere with the resolution of T85 (the triangular spectral truncation of spherical harmonics at the total wavenumber 85, that is, 256 (longitude)$\times$ 128 (latitude) grids). YY93 found that an easterly circumpolar vortex tends to emerge spontaneously in a decaying turbulent flow on a rotating sphere especially when the rotation rate is high.

A full spherical version of the forced turbulence was investigated quite recently by Nozawa and Yoden (1997a, b) in the same way as Williams (1978) but with the resolution T199 (600×300 grids). They reconfirmed the spontaneous formation of the band structure of the zonal flow. Moreover, they found that, similarly to the decaying turbulence cases, an easterly circumpolar vortex tends to appear. The property of the forced nondivergent turbulent flow on a rotating sphere may be understood through the property of the decaying turbulent flow.

However, there remains a concern about the results of YY93. As will be described below, the flows obtained by YY93 are not very turbulent especially when the rotation rate of the system is large. The initial condition used in YY93 contains, when the rotation rate is large, a large part of energy in the large scales where the linear rotation term dominates the nonlinear inertial term. On the other hand, YY93 shows that the circumpolar easterly flow appears clearer as the increase of the rotation rate. The results might be altered when the resolution of the model is increased to to represent the full nonlinear upward energy cascade of two dimensional turbulence.

In the followings, we will describe the formation of circumpolar easterly vortex in YY93 from the framework of weak nonlinear Rossby wave property on a sphere. We will then demonstrate some of the results of further numerical experiments with a high-resolution model (T341 = 1024×512) to see the pattern formation due to the real inverse cascade from small scales given by some appropriate initial conditions. We will confirm the tendency of the formation of circumpolar easterly vortex even when the rotation rate is high, in addition to the spontaneous formation of the band structure of zonal flow.

2. Nondivergent Two Dimensional Flow on a Sphere

Freely-evolving two dimensional nondivergent flow on a rotating sphere is governed by the following vorticity equation:

$$\frac{\partial \zeta}{\partial t} + J(\psi, \zeta) + 2\Omega \frac{\partial \psi}{\partial \lambda} = (-1)^{p+1} \nu_{2p} \, (\Delta + 2)^p \, \zeta, \qquad (1)$$

where $\psi(\lambda, \mu, t)$ is a streamfunction field, $\zeta(\lambda, \mu, t)$ vertical component of vorticity ($\equiv \Delta\psi$), λ longitude, $\mu = \sin\phi$ sine latitude, t time, $J(A, B)$ horizontal Jacobian, Δ horizontal Laplacian. On the right hand side, hyperviscosity of the order of p is placed with a viscosity coefficient ν_{2p} for the use of numerical calculation presented later. Note that the physical quantities are nondimensionalized by the radius of the sphere a as the length scale, the rotation rate of the system Ω^* as the time scale, and the energy velocity scale U as the advection velocity scale. By this scaling, we have to consider only the motion with unit initial total energy on the rotating sphere with the unit radius and the nondimensionalized rotation rate $\Omega \equiv U\Omega^*/a$, or, the reciprocal of Rossby number.

The important quantity which characterizes two dimensional nondivergent flow on a rotating sphere is the transition wavenumber that is defined as a local wavenumber at which the magnitude of the nonlinear term is comparable to that of the linear planetary vorticity advection term (so called β term) (Rhines 1975, Vallis and Maltrud, 1993, Rhines 1994). For the system given by (1), the transition wavenumber may be written as $k_\beta = \sqrt{2\Omega\cos\phi}$,where ϕ is the latitude. The interpretation of the transition wavenumber is that turbulence dominates when the characteristic wavenumber of the flow is larger than the transition wavenumber, while Rossby waves dominate when it is smaller. On a rotating sphere, the transition wavenumber vanishes at the pole, while it is maximum at the equator, since the β effect, i.e., the linear planetary vorticity advection, is most effective at the equator. This implies that, for a disturbance with a given characteristic scale, flow becomes turbulent more easily in the polar region than in the lower latitudes. Provided that the characteristic wavenumber of the flow is $\tilde{n}$, there appears a Rossby wave dominant region around the equator between the latitudes $\phi_t = \pm\cos^{-1}(\tilde{n}^2/2\Omega)$ when the rotation late is sufficiently large.

In the numerical experiments of YY93, the value of Ω ranges from 0 to 400. The corresponding transition wavenumber ranges from 0 to 28 at the

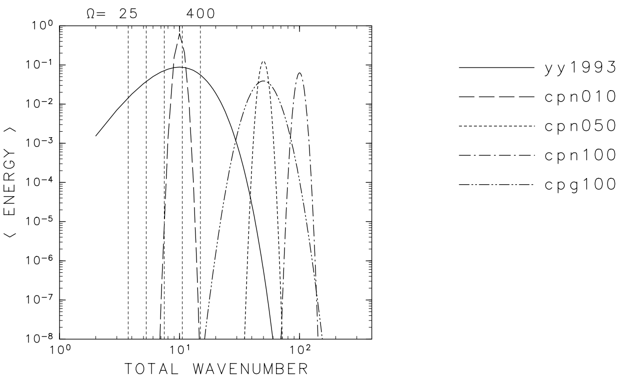

Figure 1. Five initial energy spectra. The spectral form used by YY93 is denoted by yy1993. All the other spectral forms are given by eq.(2). Five vertical dash-lines indicate the global mean transition wavenumber $n_\beta \equiv \sqrt{< k_\beta > /2\sqrt{2}} = \sqrt{\pi\Omega/(4\sqrt{2})}$ defined by Nozawa and Yoden (1997a), where $< >$ denotes global mean and the numerical factor $2\sqrt{2}$ is retained following their definition.

equator. Since the initial energy spectrum of YY93 is given by $E(n,t\!=\!0) = An^5/e^{-n/2}$, where n is the total wavenumber, the energy spectral peak is located at $n = 10$ (Fig.1), and the enstrophy spectral peak is located at $n = 12$. Thus for $\Omega > 50 \sim 100$, there appears a latitudinal regions where Rossby waves dominate in the lower latitudes. For the rapid rotation case $\Omega = 400$, the transition latitude from wavy to turbulent regime becomes $\phi_t = \pm 83°$, provided that $\tilde{n} = 10$. In this sense, the numerical flows presented by YY93 are actually not very turbulent especially when the rotation rate is large.

3. Weak Nonlinear Theory

The formation of the easterly circumpolar vortex found by YY93 may be considered as the result of turbulent mixing of the potential vorticity in the polar region where the flow regime is regarded as turbulent. On a rotating sphere, mixing of the higher potential vorticity around the pole and the lower potential vorticity of the lower latitudes causes easterly flow in the polar region, provided that there is no net positive angular momentum supply from the outside of the polar mixed region. When the rotation rate is high and the outside of the polar mixed region can be regarded as in the Rossby wave regime, it can be demonstrated that the net angular momentum supply from the outside of the polar mixed region is negative (easterly). As is expected from the knowledge that the pseudo angular momentum associated with Rossby wave is negative, the issue is to find out whether the polar mixed region absorbs Rossby waves from the wavy region to gain easterly momentum or radiates Rossby waves toward the wavy region to gain westerly momentum.

Let us consider the weak nonlinear version of the basic system (1) to investigate the wave mean-flow interaction of Rossby waves on a sphere. The amplitude expansion around a zonal mean basic state $\overline{u}(\phi)$ gives the first order linearized equation as

$$\begin{aligned} \frac{\partial\zeta'}{\partial t} + \frac{\overline{u}}{\cos\phi}\frac{\partial\zeta'}{\partial\lambda} + \frac{\hat{\beta}}{\cos\phi}\frac{\partial\psi'}{\partial\lambda} = f', \\ \hat{\beta} \equiv 2\Omega\cos\phi - \frac{\partial}{\partial\phi}\left[\frac{1}{\cos\phi}\frac{\partial}{\partial\phi}\cos\phi\overline{u}\right], \end{aligned} \tag{2}$$

where f' is the viscous dissipation term, $'$ and $\bar{}$ denote the first order and the zonal mean, respectively. The second order conservation law of the first order quantity can be derived immediately from (2):

$$\begin{aligned} \frac{\partial}{\partial t}\mathcal{A} + \nabla\cdot\mathcal{F} = \frac{\cos\phi}{\hat{\beta}}\zeta' f' \\ \mathcal{A} \equiv \frac{\zeta'^2}{2}\frac{\cos\phi}{\hat{\beta}} \\ \mathcal{F} \equiv +\left(\overline{u}\mathcal{A} + \frac{1}{2}\cos\phi(v'^2 - u'^2), \cos\phi u'v'\right), \end{aligned} \tag{3}$$

where u' and v' is the first order velocity component, and $\nabla\cdot$ is spherical divergence operator. The angular momentum conservation law is more useful as the second order zonal mean equation:

$$\frac{\partial}{\partial t}(\overline{u^{(2)}}\cos\phi) - \overline{v'\zeta'}\cos\phi = \overline{f^{(2)}}, \tag{4}$$

where $f^{(2)}$ is the viscous dissipation term. Combined with the zonal mean of (3) with the relation $\overline{\nabla\cdot\mathcal{F}} = \cos\phi\overline{v'\zeta'}$, (4) yields

$$\frac{\partial}{\partial t}\left[\overline{u^{(2)}}\cos\phi + \overline{\mathcal{A}}\right] = \cos\phi\overline{f^{(2)}} + \frac{\cos\phi}{\hat{\beta}}\overline{\zeta' f'}. \tag{5}$$

The important character of the Rossby waves propagating on a sphere is that the second order conserved quantity associated with a wave packet is $\mathcal{A}$ as shown in (3), and the related mean quantity is easterly angular momentum as shown in(5). When the rotation late is range and the effect of $\overline{u}$ can be neglected, WKBJ theory of Rossby wave propagation on a sphere (Hoskins and Karoly, 1981; Hayashi and Matsuno 1984) shows that

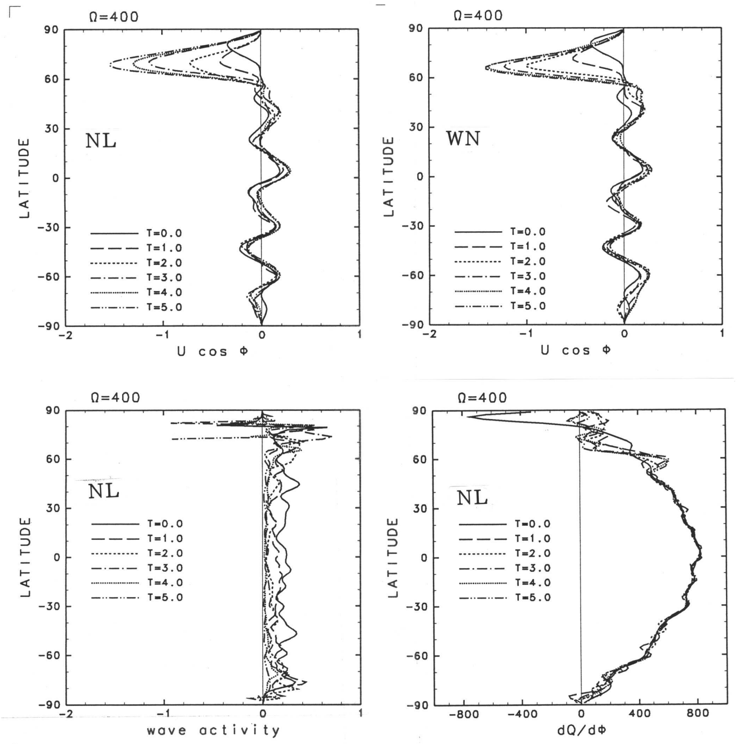

Figure 2. The comparison between the nonlinear (upper left) and weak nonlinear (upper right) evolutions of the angular momentum starting from the same initial value for the case of $\Omega = 400$. Also shown are $\overline{\mathcal{A}}$ (lower left) and $\hat{\beta}$ (lower right) of the nonlinear calculation. The numerical model utilized is the same as YY93 (T85) and hence, these figures except for the upper right represent one of the realizations in YY93 $\Omega = 400$ cases.

a Rossby wave packet propagates along a great circle seeing from the frame of rotation with the speed of eastward phase velocity of the wave packet. Let us assume a wave packet whose pitch angle at the equator is sufficiently large so that it can propagate into the higher latitudes where β is small. The propagation of Rossby wave packet induces the second order easterly flow $\overline{u^{(2)}}$, whose magnitude is enhanced in the higher latitude because of the factor $\cos\phi$, since the angular momentum associated with the wave packet is conserved during its propagation. If we allow the wave mean-flow interaction, we can expect that the large easterly fluctuation of zonal mean flow in the higher latitudes enhances the critical latitude absorption there, which contributes the easterly angular momentum accumulation in the higher latitudes.

In order to confirm the weak nonlinear scenario mentioned above, we have carried out a numerical comparison between the nonlinear and weak nonlinear evolutions starting from one of the same initial values with the same T85 model utilized by YY93. The weak nonlinear system is composed of eqs. (2) and (4) but with $\overline{u^{(2)}}$ replaced by $\overline{u}$ in (4); $\overline{u}$ is now a function of t and ϕ. Fig.2 shows a typical example of the comparative result where the accumulation of the easterly angular momentum in the polar region occurs very similarly. Once the easterly acceleration starts in the polar region, it continues steadily. The growth of easterly seems to be a little faster for the weak nonlinear evolution.

In the experiments of YY93, the spatial distribution of the amplitude of initial disturbance is statistically uniform on the sphere. When the rotation rate is large, since $\hat{\beta} \sim \beta = 2\Omega\cos\phi$, we have $\overline{\mathcal{A}} \sim \overline{\zeta'^2}/4\Omega$ (Fig.2 lower panels). This means that the initial distribution of $\overline{\mathcal{A}}$ is also statistically uniform on the sphere, which can be observed in Fig.2(lower left). Singularity appears only in the higher latitudes corresponding to the regime transition from the Rossby wave of the lower latitudes to the turbulent, or, the occurrence of critical latitude absorption and strong wave-mean flow interaction from the weak nonlinear sense. As time goes on, the amount of $\overline{\mathcal{A}}$ gradually decreases except for the singular polar region and correspondingly the westerly angular momentum increases slightly and uniformly in the mid and lower latitudes.

According to our comparative calculations, the weak nonlinear versions resemble the full nonlinear results of YY93 for the cases of $\Omega = 400$ quite well, and $\Omega = 200$ fairly well. However, the cases with $\Omega = 100$, the evolution of mean flow is occasionally different in the mid and low latitudes. For the cases of smaller values of $\Omega = 100$, there are almost no resemblance. Remember that the appearance of circumpolar vortex is not very clear in the nonlinear calculation either.

4. Results with the Higher Resolution T341

As shown in the previous section, the experiments of YY93 are not very turbulent; the appearance of the circumpolar vortex in YY93 cannot be regarded as a result of full nonlinear upward energy cascade of two dimensional turbulence. And also, as is evident from Fig.2 there are not clear spontaneous evolution of the band structure of zonal mean flow When the rotation rate is large ($\Omega = 400$), a strong development of zonal mean flow occurs only in the polar region. In the mid and low latitudes, the initial zonal mean flow does not change greatly, although latitudinally uniform westerly mean flow acceleration occurs.

Now, we will present some of the results obtained by the higher resolution model (T341 = 1024 × 512). The experiments are performed to

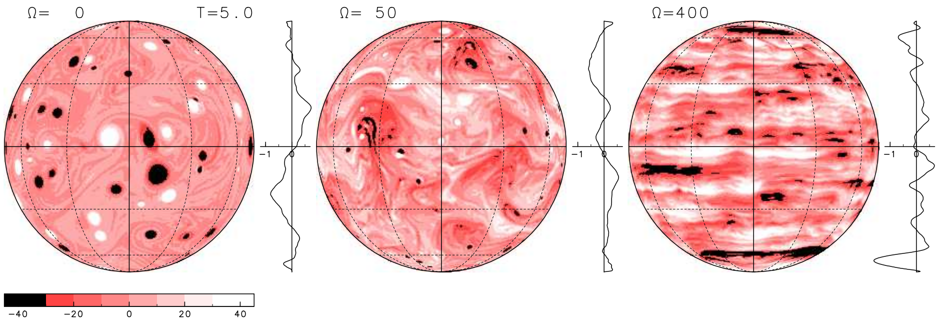

Figure 3. Vorticity fields at $t = 5$ of the cpn050 experiment for $\Omega = 0$ (left), $\Omega = 50$ (center), and $\Omega = 400$ (right) with the T341 model. Orthographic projection from $\lambda = 0°$, $\phi = 0°$ is used and lines of meridians and parallels are drawn for every 30°. Solid line on the right side of each panel shows the zonal mean zonal angular momentum as a function of sine latitude.

confirm the emergence of the circumpolar vortex and to observe the formation of band structure even from the initial spectral profile which does not contain spectral energy in the Rossby wave regime.

The new initial energy spectrum is given by $E(n, t=0) = An^{\gamma/2}/(n + n_0)^{\gamma}$. Following the normalization utilized by YY93, A is given by the condition $\sum_{n=2}^{N} E(n, t=0) = 1$ (the total kinetic energy is unity). The initial complex amplitudes of the spherical harmonics expansion of the stream function are determined so that they have random amplitude and phase under the above restriction. In Fig.1, four sets of the energy spectra utilized in our experiments are presented. The values of (n_0, γ) are (10,1000) for cpn010, (50,1000) for cpn050 (the standard set), (100,1000) for cpn100, and (50,100) for cpg100.

Ten initial conditions are made with different random numbers for each experimental set. The hyper-viscosity is set with $p = 8$ and $\nu_{2p} = 1 \times 10^{-38}$. Time evolutions are computed until $t = 5$ by the fourth-order Runge-Kutta method with the time increment of $\Delta t = 1 \times 10^{-3}$.

Fig.3 is an example of the vorticity fields at $t = 5$ evolved from the same initial condition of the spectral type cpn050 but with the different value of Ω. In the non-rotational case (left), a number of coherent vortices appear and then their population decreases gradually through mergers. The amount of zonal mean angular momentum plotted in the right hand side of

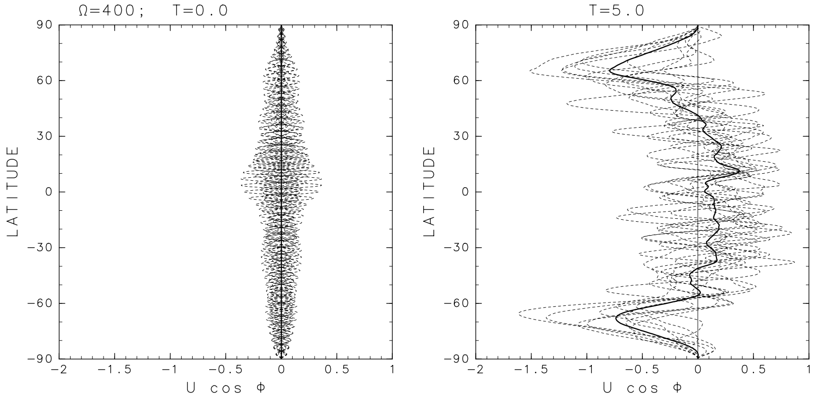

Figure 4. Dashed lines represent the zonal mean angular momentum distributions of the 10 initial conditions of cpn050 (left) and their final profiles at $t = 5$ (right) for $\Omega = 400$ with the T341 model. Thick lines represent the ensemble average of those dashed lines.

the panel may seem to be very large, but the profile changes as the coherent vortices move. In the high-rotation case $\Omega = 400$(right), the vorticity field shows zonally elongated structures. The profile of the zonal mean angular momentum shows the emergence of easterly circumpolar vortex, particularly in the southern hemisphere for this run. In addition to that, the zonal band structure appear in the mid and low latitudes. As will described below, the zonal band structure of $\Omega = 400$ obtained by this T341 experiment is not just a remainder of the initial zonal profiles as that of T85 experiment of YY93.

Fig.4 shows the statistical feature of the latitudinal distributions of zonal mean angular momentum. 10 initial conditions of cpn050 and those at $t = 5$ (right) for $\Omega = 400$ are plotted. It is clearly observed that the circum polar easterly vortex appears statistically through the nonlinear energy upward cascade from the initial spectral peak located at wavenumber 50. The latitudinal distribution of the zonal mean angular momentum of each realization is different to each other. However, there seems to be a typical latitudinal wavenumber of zonal mean flow roughly proportional to n_β (Fig.6). The characteristics observed in YY93 and considered by the weak nonlinear theory still appear even with this turbulent initial condition; Strong easterly appears in the high latitudes while weak westerly appears in the mid and low latitudes. This tendency can be more clearly observed in the ensemble average profile, where the rapid latitudinal variation of the angular momentum profile of each realization is smoothed out.

Fig.5 shows the dependence of the zonal mean zonal angular momentum

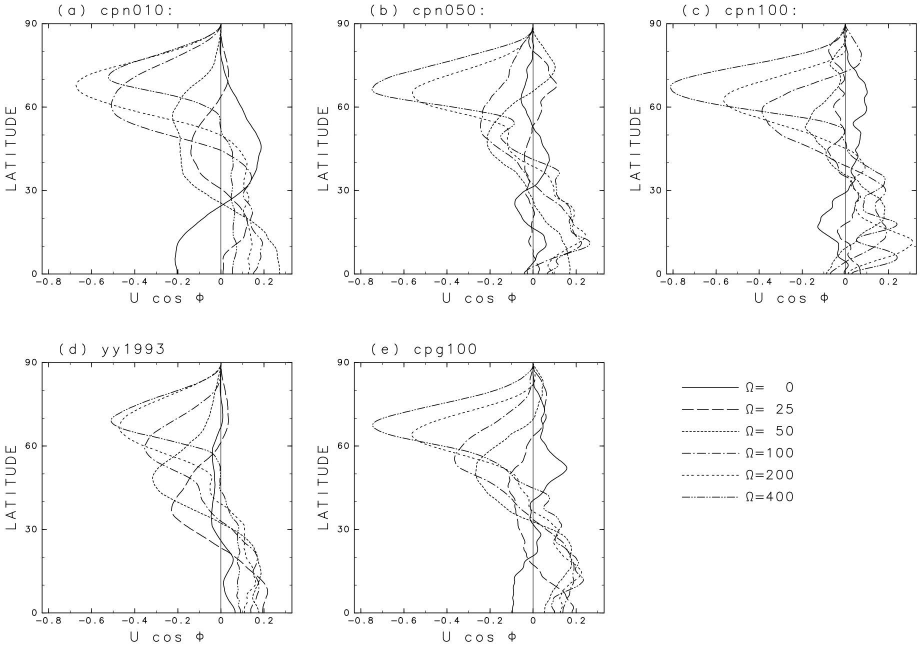

Figure 5. Dependence of zonal mean angular momentum on the rotation rate Ω for the five sets of the different initial spectral profiles. Ensemble average of 2×10 runs under the assumption of equatorial symmetry.

at $t = 5$ on Ω for the five experimental sets with the different initial spectral profiles. The formation of the easterly circumpolar vortex for large Ω is a robust result independent of the choice of the initial energy spectrum. As Ω increases, the intensity of the easterly vortex becomes large and its maximum position shifts toward the higher latitudes. Note that the easterly vortex for $\Omega = 400$ is stronger for the larger value of n_0 from the set cpn010 to cpn100. As a result of the ensemble average, westerly flow appears in the lower latitudes for large Ω cases. However, as mentioned previously each realization shows a zonal band structure in mid and low latitudes. The ensemble average masks the band structure because the latitudinal position of the jets dependent rather randomly on each realization.

Fig.6 shows the time evolution of the zonal mean angular momentum for various values of Ω starting from the same initial value of the energy spectral form cpn050. The band structure of the zonal angular momentum can be clearly observed as the increase of Ω. The development of the band structure occurs rather early stage of the time evolution. At the beginning of the integration, the zonal angular momentum profile has a rather high characteristic latitudinal wavenumber, since the initial spectral peak is lo-

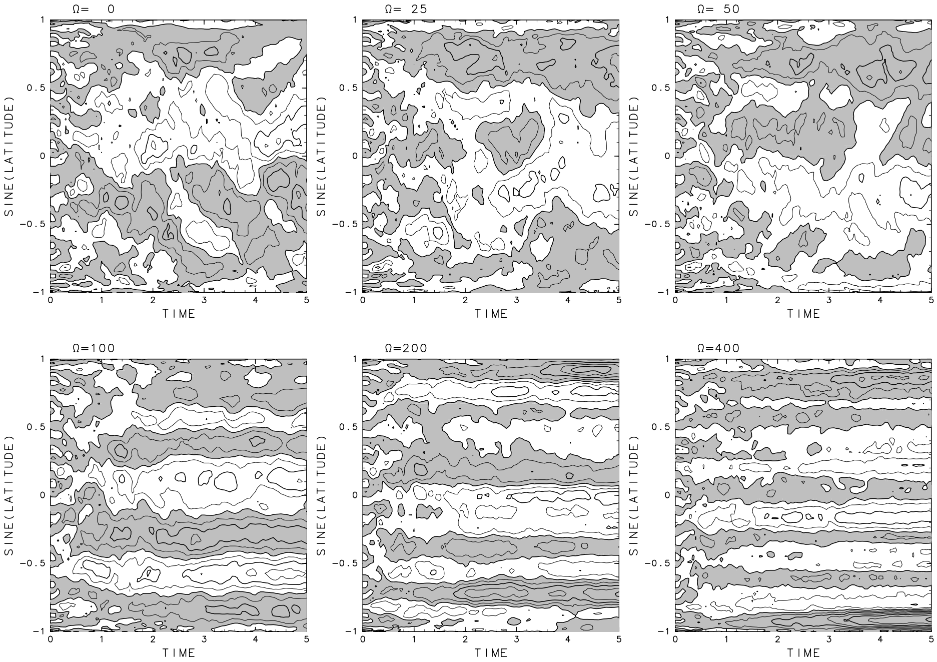

Figure 6. The time evolutions of zonal mean angular momentum from the same initial condition of cpn050 but for the different values of Ω.

cated at $n = 50$. The characteristic wavenumber evolves rapidly toward the lower wavenumber. Around $t \sim 0.5$, the band structure comes to a steady or very slowly evolving state. As reported by Nozawa and Yoden (1997a) for the forced two dimensional turbulence on a sphere, the characteristic wavenumber of the zonal band profile seems to be roughly proportional to n_β.

Fig.7 shows the time evolution of the zonal mean angular momentum for the case of $\Omega = 400$ starting from the three different initial energy spectral profiles cpn010, cpn050, and cpn100. Note that the time scale is different from Fig.6; log time scale is adopted. As is discussed in the previous section, when the initial spectral peak is located in the spectral range of Rossby wave regime ($n_0 < k_\beta(\phi = 0)$), the zonal band structure is almost completely determined by the initial zonal band profile (cpn010, Fig.7 left). However, when the initial energy profile has the spectral peak located in the turbulent regime ($n_0 \gg k_\beta(\phi = 0)$), a spontaneous evolution of the zonal band structure occurs (cpn050 and cpn100, Fig.7 center and right). Fig.7 indicates clearly that the band structure establishes as the spontaneous evolution of the nonlinear upward cascade of energy.

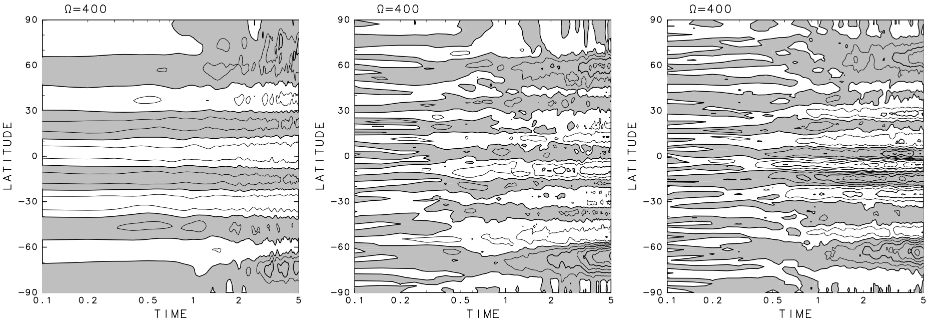

Figure 7. The time evolution of zonal mean angular momentum for $\Omega = 400$ starting from cpn010 (left), cpn050 (center), and cpn100 (right). Note that the time scale is plotted by the log scale.

The rapid change of the energy spectrum also occurs at rather early stage of the time evolution (not shown). This should be directly related to the establishment of the band structure at around $t \sim 0.5$. The distribution of the energy spectrum is characterized by the appearance of anisotropy. The two dimensional energy spectrum at $t = 5$ is shown in Fig.8. The energy density of small m is dominant in the range of $n < k_\beta(\phi = 0)$ while the energy is very small in an airfoil-shaped region at the lower edge in the wavenumber space (m, n) as found in the forced turbulence experiments Nozawa and Yoden (1997a,b). The existence of such a small energy region is qualitatively explained by the analogy of a dumbbell region obtained in the β-plane experiment by Vallis and Multrad (1993). Anisotropic distribution of the energy is also found in the high total-wavenumber region $n > k_\beta$; energy is confined in the region of small zonal wavenumber m.

5. Concluding remarks

The spontaneous appearance of circumpolar easterly vortices reported by YY93 was interpreted by the Rossby wave property from the framework of weak-nonlinear theory. The initial energy spectral peak adapted there is located almost in the range of wave regime especially when the rotation rate

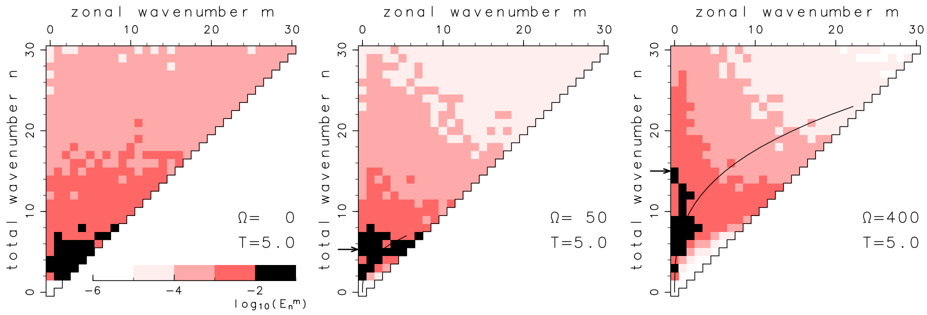

Figure 8. Two dimensional energy spectrum at $t = 5$ of the cpn050 experiment for $\Omega = 0$ (left), $\Omega = 50$ (center), and $\Omega = 400$ (right) with the T341 model. The air foil region determined by Nozawa and Yoden (1997b) is denoted by thick line.

is large, which justifies the explanation of angular momentum redistribution by Rossby waves. A series of new experiments with the higher resolution T341 and new sets of initial energy spectral distributions are performed to give the following results:

1. The circumpolar easterly vortices appear in high latitudes and the zonal band structures of alternating mean zonal jets appear in mid and low latitudes even after the full nonlinear upward cascade of turbulent energy for high-rotation cases.
2. The formation of the easterly circumpolar vortex is a robust feature of the two dimensional decaying turbulence on a rotating sphere and insensitive to the choice of the initial energy spectrum.
3. The zonal band structures are discernible from an early stage of the time evolution, and once established their latitudinal positions are hardly changed with time. The number of the jets increases while the width of them decreases as the rotation rate increases.
4. Two dimensional energy spectrum shows anisotropy due to the rotation effect of the sphere. An airfoil shape with very small energy density appears in low total-wavenumber region. Anisotropic distribution of the energy is also found in the high total-wavenumber region.

* * *

The GFD-DENNOU Library (SGKS Group 1995) was used for drawing the figures. Numerical calculation was done on VPP500/15 at the Data Processing Center, Kyoto University. This work was supported in part by the Grant-in-Aid for Scientific Research of the Ministry of Education, Science, Sports and Culture of Japan and by the Grant-in-Aid for the Research for the Future Program "Computational Science and Engineering" of the Japan Society for the Promotion of Science.

REFERENCES

SGKS Group, 1995: DCL-5.1. http://www.gfd-dennou.org/library/dcl/; GFD-Dennou Club (in Japanese).

Hayashi, Y.-Y. and Matsuno, T., 1984: Amplitude of Rossby wavetrains on a sphere. *J. Met. Soc. Japan,* **62**, 377-387.

Hoskins, B.J. and Karoly, D.J., 1981: The steady linear response of a spherical atmosphere to thermal and orographic forcing. *J. Atmos. Sci.*, **38**, 1179-1196.

Nozawa, T. and Yoden, S., 1997a: Formation of zonal band structure in forced two-dimensional turbulence on a rotating sphere. *Phys. Fluids*, **9**, 2081-2093.

Nozawa, T. and Yoden, S., 1997b: Spectral anisotropy in forced two-dimensional turbulence on a rotating sphere. *Phys. Fluids*, **9**, 3834-3842.

Rhines, P.B., 1975: Waves and turbulence on a beta-plane. *J. Fluid Mech.*, **69**, 417-443.

Rhines, P.B., 1994: Jets. *Chaos*, **4**, 313-339.

Vallis, G.K. and Maltrud, M.E., 1993: Generation of mean flows and jets on a beta plane and over topography. *J. Phys. Oceanogr.*, **23**, 1346-1362.

Williams, G.P., 1978: Planetary circulations: 1. Barotropic representation of Jovian and Terrestrial turbulence. *J. Atmos. Sci.*, **35**, 1399-1426.

Yoden, S. and Yamada, M., 1993: A numerical experiment on two-dimensional decaying turbulence on a rotating sphere. *J. Atmos. Sci.*, **50**, 631.